Journal of Nuclear Medicine, published on April 27, 2017 as doi:10.2967/jnumed.116.189035

SSTR-mediated Imaging In Breast Cancer: Is There A Role For Radiolabeled Somatostatin Receptor Antagonists?

Simone U. Dalm[1], Joost Haeck[1], Gabriela N. Doeswijk[1], Erik de Blois[1], Marion de Jong[1] and Carolien H.M. van Deurzen[2]

[1]Department of Radiology & Nuclear medicine, Erasmus MC, Rotterdam, The Netherlands

[2]Department of Pathology, Erasmus MC, Rotterdam, The Netherlands

Corresponding author:

Simone Dalm

Room: Na2510

P.O box 2040

3000 CA Rotterdam, the Netherlands

+31-107041033

s.dalm@erasmusmc.nl

Word count: 4760

Running title: BC imaging using a SSTR antagonist

ABSTRACT

INTRODUCTION:

Recent studies showed enhanced tumor targeting by novel somatostatin receptor (SSTR) antagonists compared to clinically widely used agonists. However, these results have mostly been obtained in neuroendocrine tumors and only limited data is available for cancer types with lower SSTR expression, including breast cancer (BC). To date, only two studies reported higher binding of the antagonist versus the agonist in BC, but in both studies a limited number of cases were evaluated. In this pre-clinical study, we further investigated whether the application of a SSTR antagonist could improve SSTR-mediated BC imaging in a large panel of BC specimens. We also generated an in vivo BC mouse model and performed single-photon emission computed tomography/Magnetic resonance imaging (SPECT/MRI) and biodistribution studies.

MATERIALS AND METHODS:

^{111}In-DOTA-Tyr^{3}-octreotate (SSTR agonist) and ^{111}In-DOTA-JR11 (SSTR antagonist) binding to 40 human BC specimens was compared using in vitro autoradiography. SSTR2-immunostaining was performed to confirm SSTR2 expression of the tumor cells. Furthermore, binding of the radiolabeled SSTR agonist and antagonist was analyzed in tissue material from 6 patient derived xenografts (pdx's). One pdx, the estrogen receptor positive model T126, was chosen to generate in vivo mouse models containing orthotopic breast tumors for in vivo SPECT/MR imaging and biodistribution studies after injection with ^{177}Lu-DOTA-Tyr^{3}-octreotate or ^{177}Lu-DOTA-JR11.

RESULTS:

^{111}In-DOTA-JR11 binding to human BC tissue was significantly higher than ^{111}In-DOTA-Tyr^{3}-octreotate binding ($p<0.001$). The median (interquartile range) ratio of the antagonist versus the agonist binding was 3.39 (2-5)). SSTR2-immunostaining confirmed SSTR2 expression in the tumor cells. SPECT/MR imaging performed in the mouse model resulted in better tumor visualization with the antagonist. This was in line with the significantly higher tumor uptake of the radiolabeled antagonist versus the agonist measured in the biodistribution studies 285 min post injection of the radiotacers (1.92±0.43 versus 0.90±0.17 %ID/g tissue ($p=0.002$), respectively).

Conclusion: SSTR antagonists are promising candidates for BC imaging.

Keywords: Breast cancer, Imaging, Somatostatin receptor, Agonist, Antagonist

INTRODUCTION

Receptor-mediated nuclear imaging is successfully applied in the clinic in patients with neuroendocrine tumors. For this purpose, radiolabeled SSTR agonists are used that target SSTRs overexpressed on tumor cells. In 1990, Reubi et al. (*1*) reported SSTR expression in 21-46% of BC specimens studied by in vitro autoradiography. Since then, multiple clinical studies targeting these receptors for imaging purposes were performed. However, due to conflicting results (sensitivity and specificity ranged from 36%-100% and 22%-100%, respectively (*2*)), SSTR-mediated nuclear imaging is currently not routinely used in BC patients. Low and heterogeneous SSTR expression seems to be the main reason for unsuccessful tumor targeting, as described in our recently published review article (*2*). Therefore, novel developments within the field of nuclear medicine are needed in order to improve SSTR-mediated imaging of BC, to ultimately provide a role for this method in BC patient care.

A promising development in the field of SSTR-mediated imaging is the application of SSTR antagonists. Enhanced tumor targeting of receptor antagonists versus receptor agonists is counterintuitive, since agonists can be internalized which leads to accumulation of radioactivity in cells. However, Ginj et al. (*3*) reported that SSTR antagonists bind to more binding sites than agonists. Based on the results of recent studies demonstrating enhanced tumor targeting of neuroendocrine tumors with SSTR antagonists (*3*-*7*), the ability of the antagonist to bind to more binding sites could be more important than internalization of SSTR agonists. This is consistent with a clinical pilot study performed by Wild et al. (*7*) who reported a 1.7-10.6 times higher tumor dose with the SSTR antagonist ^{177}Lu-DOTA-JR11 compared to the SSTR agonist ^{177}Lu-DOTA-Tyr^3-octreotate. The above-mentioned studies are mainly based on neuroendocrine tumors. However, the use of this enhanced binding of radiolabeled SSTR antagonists might especially be interesting for targeting cancer types with a lower SSTR expression, such as BC. Cescato et al. (*4*) and Reubi et al. (*8*) demonstrated higher binding of SSTR antagonists versus SSTR agonists to BC tissue in vitro. However, these promising results were based on the evaluation of tissue from 7 and 13 breast carcinomas, respectively. Therefore, the aim of the current study was to further investigate whether the use of SSTR antagonists could provide novel possibilities for SSTR-mediated imaging of BC. To do so, binding of the radiolabeled SSTR agonist (^{111}In-DOTA-Tyr^3-octreotate) and the SSTR antagonist (^{111}In-

DOTA-JR11) to a large panel of human BC specimens was compared. Furthermore, we generated a suitable BC xenograft mouse model and performed preliminary SPECT/MRI and biodistribution studies after injection of ^{177}Lu-DOTA-JR11 or ^{177}Lu-DOTA-Tyr^{3}-octreotate.

MATERIALS AND METHODS

Radioligands

The SSTR agonist, DOTA-Tyr^{3}-octreotate (BioSynthema) and the SSTR antagonist, DOTA-JR11 (kindly provided by Dr. Helmut Maecke), with high SSTR2 affinity were used (Table 1). The radiotracers were radiolabeled with ^{111}In (Covidien) or ^{177}Lu (IDB Holland bv) as previously described (*9*). Specific activity was 80 and 100 MBq/nmol for the ^{111}In and ^{177}Lu labeled peptide analogs, respectively. Radiometal incorporation and radiochemical purity were >90%.

Human BC Specimens

Fresh frozen tissue specimens from 40 human BCs (31 ductal carcinomas, 4 lobular carcinomas and 5 other subtypes) were selected from the Erasmus MC tissue bank for autoradiography studies comparing SSTR agonist and antagonist binding. The majority of the cases were positive for estrogen receptor (ER; 75%), progesterone receptor (PR; 55%) and negative for human epidermal growth factor 2 (HER2; 18%). The study adhered to the Code of Conduct of the Federation of Medical Scientific Societies in The Netherlands.

In Vitro Autoradiography

Fresh frozen tissue sections (10 µm) were incubated for 1.5 h with 100 µL 10^{-9} M ^{111}In-DOTA-Tyr^{3}-octreotate or ^{111}In-DOTA-JR11, with or without 10^{-6} M octreotide as a control for receptor specificity. Following incubation, the excess radiotracer was removed and tissue sections were exposed to super resolution phosphor screens (Perkin Elmer) for 3 d, after which screens were read using the Cyclone (Perkin Elmer). Binding of the radiotracers to tumor containing regions, identified by hematoxylin and eosin stainings of adjacent tissue sections, was quantified using OptiQuant software (Perkin Elmer) and expressed as digital lights units per mm^2 (DLU/mm^2). Quantified uptake was corrected for non-specific binding by subtracting DLU/mm^2 of the blocked sections from DLU/mm^2 of the unblocked sections (DLU/mm$^2_{net}$ = DLU/mm^2 $_{total}$ – DLU/mm^2 $_{blocked}$). Drops containing 1 µL 10^{-9} M of the radiotracers were

used as standards to determine the added dose (DLU/$mm^2_{standards}$×100). Tumor-bound radiotracer was expressed relative to the added dose (%AD).

SSTR2 Immunostaining

SSTR2-immunostaining was performed on fresh frozen tumor tissue, using the Ventana Benchmark Ultra automated staining system (Ventana Medical System) according to manufacturer's instructions. The tissue sections were fixed for 1 h in neutral buffered formalin and washed in PBS prior to immunostaining. Subsequently, antigen retrieval, immunostaining for SSTR2 (BIO-TREND, SS-8000-RM-1, dilution: 1:50, 120 min at 36 °C), amplification, detection and visualization was performed using the Ultra Cell Conditioning Solution CC2, Ultraview amplification kit and Ultraview Universal DAB detection kit (all from Ventana Medical Systems). The immunostained sections were contra stained with hematoxylin. An experienced pathologist (CvD), blinded for histopathological tumor information (e.g. ER, PR and HER2 status) and autoradiography results, scored the stained sections on intensity (negative, weak, moderate, strong) and heterogeneity (homogenous versus heterogeneous expression).

Mouse Model, SPECT/MRI and Biodistribution

All animal experiments were approved by the Animal Welfare Committee and conducted in accordance to accepted guidelines.

In order to select an appropriate in vivo mouse model a panel of 6 excised tumors from patient derived xenografts with varying hormone receptor expression was tested for their ability to bind the agonist and the antagonist using autoradiography studies. Subsequently, one xenograft that showed high radiotracer binding was chosen to create an in vivo model for imaging and biodistribution studies. Preferably, this model should be ER-positive, since ER-positive BC seems to be the most promising BC subtype for SSTR-mediated imaging based on previously published studies that demonstrated that high SSTR2 expression was associated with ER-positive BC (*10-12*).

For the in vivo studies, Balb c nu/nu female mice containing estrogen receptor (ER)-positive T126 pdx's were used. To generate this model, small tumor pieces (~6 mm^3) from a donor animal were transplanted in the 4^{th} mammary fat pad of Balb c nu/nu female mice supplemented with 4 mg/L ß-

estradiol. The initial generation of the patient derived xenograft model was performed as described by Marangoni et al. (*13*)

When tumors were of sufficient size (≥ 200 mm^3), animals received an intravenous injection of ~20 MBq/200 pmol ^{177}Lu-DOTA-Tyr^3-octreotate or ^{177}Lu-DOTA-JR11 (n=6 animals per radiotracer). SPECT/MRI was performed 240 min after radiotracer injection, while animals were anesthetized using isoflurane/O_2 and body temperature was maintained. Focused SPECT images were acquired using a 4-head multipinhole system (NanoScan SPECT/MRI, Mediso Medical Imaging) in 30 min (28 projections, 60 s/projection). Images were reconstructed using the ordered subset expectation maximization method with 6 iterations. Concerning MRI, T1 and T2 images were acquired using a gradient echo sequence (TR/TE=12/2 ms) and a spin echo sequence (TR/TE=4500/52 ms). Other scan parameters were: field of view: 70 mm, matrix: 128×128 and slice thickness: 1 mm. The MR images were used to assess tumor composition. Image quantification was performed using the scanner software (Nucline (version 3), Mediso Medical Imaging). A region of interest was drawn around the tumor in T2 weighted MR images, which best showed the tissue boundaries. The total SPECT uptake within the region of interest was divided by the tumor volume to give a volumetric uptake (KBq/ml) which could be compared between subjects.

After imaging (t=285 min post injection), animals were euthanized, organs and tumors were excised, weighed and counted in an automatic γ-counter (1480 WIZARD, PerkinElmer) to determine radioactivity uptake. Standards containing 10 µL of the injected activity were also counted in the γ-counter to determine the injected dose. Subsequently, tumor and organ uptake relative to the injected dose were calculated and expressed as the percentage of injected dose per gram tissue (%ID/g tissue). To determine specificity of radiotracer uptake, an additional group of animals (n=2 for each radiotracer) was injected with 2 MBq/200 pmol ^{177}Lu-DOTA-JR11 or ^{177}Lu-DOTA-Tyr^3-octreotate plus 40 nm unlabeled DOTA-JR11 or DOTA-Tyr^3-octreotate, respectively, and biodistribution studies were performed at the same time point post injection (285 min) as animals that were scanned.

For the γ-counter measurements, a radionuclide specific energy window, a counting time of 60 s and a counting error <5% were used for γ-counter measurements.

Statistics

Grahpad Prism 5 was used for statistical analyses. The Wilcoxon signed rank test was used to compare the Net %AD of the radiotracers in human BC samples. To compare radioligand binding of ER, PR and HER2 positive versus negative samples and to compare in vivo radiotracer uptake in the tumor xenografts and tumor to organ ratios, the Mann Whitney test and the unpaired t test were used. $P<0.05$ were considered statistically significant.

RESULTS

In Vitro Autoradiography and SSTR2-immunostaining of Human BC Specimens

The results of the in vitro autoradiography experiment were quantified. The Net %AD of the antagonist bound to the BC specimens was significantly higher ($p<0.001$) than that of the agonist (Fig. 1). Amongst the receptor positive tumors (38/40), the ratio %AD antagonist to %AD agonist ranged from 1 (only 1 case) to 57 (median (interquartile range) = 3.39 (2-5)).

There was no significant association between the %AD of ^{111}In-DOTA-JR11 or ^{111}In-DOTA-Tyr^3-octreotate with ER status (p=0.2 and 0.8, respectively), PR status (p=0.3 and 0.1, respectively) or HER2 status (p=0.2 and 0.09, respectively).

SSTR2-immunostaining confirmed SSTR2 expression on the majority (37/40) of BC specimens (Fig. 1A). Two specimens that were negative with immunohistochemistry, were also negative on autoradiography. One specimen was negative on SSTR2-immunostaining and positive on autoradiography but the Net %AD was low. The results of scoring the SSTR2-positive tumors on intensity and heterogeneity are displayed in Table 2.

In Vitro Autoradiography of the BC Pdx's

Six excised tumors from BC pdx's were tested for agonist and antagonist binding (Fig. 2). Antagonist binding was clearly higher for 3/6 xenografts (T126, T283 and T250), while low binding was observed in the remaining xenografts. Two xenografts showed relatively high ^{111}In-DOTA-JR11 and ^{111}In-DOTA-Tyr^3-octreotate binding (T126 and T283) and were suited for in vivo experiments. Finally, T126 was chosen to create an in vivo mouse model.

SPECT/MRI and Biodistribution Studies

The images acquired with ^{177}Lu-DOTA-Tyr^3-octreotate and ^{177}Lu-DOTA-JR11 are displayed in Fig. 3A+B. The T1 and T2 MR images showed homogenous signal intensity throughout the tumor, indicating viability. Significantly higher radioactivity uptake of ^{177}Lu-DOTA-JR11 versus ^{177}Lu-DOTA-Tyr^3-octreotate was observed on the SPECT scans (1.12±0.4 %ID/mL vs 0.8±0.1 %ID/mL respectively,

p<0.05). Hematoxylin and eosin staining and SSTR2-immunostaining demonstrated SSTR2 expression on the tumor (Fig. 3C+D).

In line with SPECT/MRI results, biodistribution studies resulted in a significantly higher tumor uptake of the antagonist versus the agonist (p=0.022). High ^{177}Lu-DOTA-JR11 and ^{177}Lu-DOTA-Tyr^3-octreotate uptake was also observed in the pancreas (4.09±1.67 and 2.57±1.64 %ID/g tissue, respectively) and kidneys (12.29±4.61 and 10.06±3.42 %ID/g tissue, respectively). There was no significant difference in tumor to pancreas (0.58±0.39 versus 0.55±0.39, p=0.82) and tumor to kidney (0.18±0.09 versus 0.10±0.04, p=0.09) ratio with ^{177}Lu-DOTA-JR11 versus ^{177}Lu-DOTA-Tyr^3-octreotate, respectively. This was also the case for tumor to blood and tumor to muscle ratio, which was ≥ 3.0 in all cases.

Injection of ^{177}Lu-DOTA-JR11 or ^{177}Lu-DOTA-Tyr^3-octreotate plus an excess of unlabeled DOTA-JR11 or DOTA-Tyr^3-octreotate, respectively, significantly blocked tumor uptake, demonstrating SSTR specificity of radiotracer uptake in the tumor.

The results of the biodistribution studies and the tumor to organ ratios are displayed in Fig. 4.

DISCUSSION

SSTR-mediated nuclear imaging is currently not applied for BC, due to variable results of clinical studies. However, most of these studies were performed over a decade ago, while recently major improvements have been made including the development of SSTR antagonists. Previous research demonstrated that SSTR antagonists bind to more binding sites than agonists (*3*). In BC, low and heterogeneous SSTR expression seem to be limiting factors for successful SSTR-mediated nuclear imaging (*2*). Therefore, the application of SSTR antagonists might offer novel possibilities for successful BC imaging. In this study, we compared the SSTR agonist ^{111}In-DOTA-Tyr^3-octreotate and the antagonist ^{111}In-DOTA-JR11 in 40 human BC specimens and in a BC mouse model. Since both DOTA-Tyr^3-octreotate and DOTA-JR11 have high affinity for SSTR2 and low affinity for other SSTR subtypes (Table 1), the observed difference in binding/uptake is mainly based on interaction with SSTR2 (*14,15*).

We found significant higher binding (up to 57 times higher) of ^{111}In-DOTA-JR11 versus ^{111}In-DOTA-Tyr^3-octreotate to the BC specimens. Our findings are in line with results of Cescato et al. (*4*) who demonstrated higher binding of ^{177}Lu-DOTA-BASS, another SSTR antagonist compared to ^{177}Lu-DOTA-Tyr^3-octreotate in 7 BCs analyzed by in vitro autoradiography studies. In the same study the authors also compared ^{177}Lu-DOTA-BASS and ^{177}Lu-DOTA-Tyr^3-octreotate binding to other tumor types, including pheochromocytoma's. Binding of the antagonist to BCs was as high as binding of the agonist to pheochromocytoma's. Since pheochromocytoma's are clinically successfully targeted with the agonist (*4*), this indicates the potential of targeting BC with SSTR antagonists. In a recent study Reubi et al. (*8*) compared binding of ^{125}I-JR11 and ^{125}I-Tyr^3-octreotide in BCs, also resulting in enhanced binding of the antagonist versus the agonist. In this study the authors also compared binding of the radioligands to neuroendocrine tumors, but under different experimental conditions hampering comparison with the results obtained in breast tumors.

In our autoradiography studies, a higher level of unspecific binding was observed for ^{111}In-DOTA-JR11 versus ^{111}In-DOTA-Tyr^3-octreotate. This might be due to the fact that blocking studies were performed with unlabeled octreotide, a well-known SSTR agonist, rather than an antagonist. In the in vivo blocking studies, an excess of unlabeled DOTA-JR11 was used for blocking, which demonstrated that

radiolabeled JR11 is highly specific. This was also demonstrated in studies by Reubi et al. (*8*), where the authors performed an autoradiography experiment using ^{125}I-DOTA-JR11 and added unlabeled DOTA-JR11 for blocking.

The group of BCs that we studied was heterogeneous. However, concerning subtype, the majority of the tumors were classified as ductal, ER-positive, HER2-negative carcinomas. Although this is consistent with the distribution of BC subtypes in the clinic, it limited the possibility of comparing SSTR expression, and SSTR agonist and antagonist binding across different BC subtypes, because the subgroups were too small for reliable conclusions. This probably also explains why we found no significant association with ER, PR or HER2 status and ^{111}In-DOTA-octreotate or ^{111}In-DOTA-JR11 binding in this study whereas ER and PR showed a significant positive association with SSTR expression in our previous study in which receptor expression of 684 lymph node negative BC was analyzed (*12*).

SSTR2-immunostaining confirmed the expression of SSTR2 on the tumor sections analyzed by in vitro autoradiography. The majority of the specimens (51.4%) showed weak SSTR2 expression, which is in line with previous findings (*2*). There was a discrepancy in 1 BC specimen that was negative for SSTR2-immunostaining and positive in the autoradiography experiments, the Net %AD was low though. This might be explained by variability of SSTR2 expression within a tumor. In all other cases SSTR2 expression on immunostaining matched the autoradiography results.

In vivo imaging was successful with both ^{177}Lu-DOTA-JR11 and ^{177}Lu-DOTA-Tyr^3-octreotate, although tumors were visualized better using ^{177}Lu-DOTA-JR11. In line with this, the measured ex vivo tumor uptake of ^{177}Lu-DOTA-JR11 was 100% higher than that of ^{177}Lu-DOTA-Tyr^3-octreotate, which resulted in better tumor visualization. Considering that ^{177}Lu is a therapeutic radionuclide and enhanced tumor targeting with ^{177}Lu-DOTA-JR11 was reported, the next step would be to determine whether ^{177}Lu-DOTA-JR11 could also be used for safe and effective treatment of these tumors. In line with findings of our previous study (*6*) comparing the application of ^{177}Lu-DOTA-Tyr^3-octreotate and ^{177}Lu-DOTA-JR11 for therapeutic purposes in a neuroendocrine mouse model, we expect that the enhanced in vivo tumor uptake of the antagonist in BC will also result in a better therapeutic efficacy. Thus, SSTR-mediated targeting of BC might not only offer imaging possibilities (including therapy response assessment and visualization of metastases), but also therapy options.

When using the radiolabeled antagonist for therapy, the uptake of the radiotracer in non-target organs should be taken into account. Next to the tumors, we observed high radiotracer uptake in the kidneys. However, kidney uptake can be reduced remarkably when co-injecting the radiotracers with kidney protectors e.g. modified fluid gelatin or a solution containing arginine and lysine (*16,17*). Wild et al. (*7*) reported a 6.2 times higher tumor to kidney ratio for ^{177}Lu-DOTA-JR11 versus ^{177}Lu-DOTA-Tyr^3-octreotate. In this study, patients were pre-injected with a solution of arginine and lysine, while in our preclinical in vivo study kidney protection was not applied and tumor to kidney ratio was similar for the antagonist and the agonist. Based on the results of Wild et al. (*7*), we expect that applying kidney protectors would have a positive influence on tumor to kidney ratio, which would be more in favor of the antagonist due to the higher ^{177}Lu-DOTA-JR11 uptake in the tumor.

Next to the kidneys, we observed high uptake in the pancreas. However, radiosensitivity of the pancreas is relatively low (*18*) and our previous study showed that the washout in the pancreas with the antagonist is relatively fast, a pancreas clearance half-life of 13.6 h. versus a tumor clearance half-life of 30 h in a human small cell lung cancer xenograft was found (*6*). Furthermore, the pancreas was not identified as a dose limiting organ in studies using the agonist (*19*).

Recently the results of a large phase 3 clinical trial using ^{177}Lu-DOTA-Tyr^3-octreotate for treatment of midgut neuroendocrine tumors, the NETTER1 trial, was published and reported grade 3 or 4 hematoxicological side effects, although only seen in a small percentage of the patients (*20*). In this study, where ^{177}Lu-DOTA-Tyr^3-octreotate was administered concomitantly with a renal protective agent, no renal toxicity was reported. Even though we found no significant difference in tumor to blood and tumor to kidney ratio of the radiolabeled antagonist versus the agonist, the higher absolute uptake of the radiolabeled antagonist in background organs should be kept in mind when the radioligand is applied for therapy purposes, since it can potentially have consequences. Furthermore, dosimetry studies are needed to determine whether the absolute uptake of ^{177}Lu-DOTA-JR11 in BC patients is sufficient for therapy, keeping in mind the dose limiting organs (the kidneys and the bone marrow (*19*)) for peptide receptor radionuclide therapy using SSTR radioligands.

The heterogenic expression of SSTR2 in BC is also something that should be kept in mind, especially when the radioligand is used for therapeutic purposes. With respect to this, the radionuclide

coupled to the tracers should be selected carefully. If the antagonist is coupled to a radionuclide with a good penetration range (depending on the tumor size and the level of heterogeneity, ^{90}Y might be more favorable than ^{177}Lu because of its deeper penetration range), it is expected that radiation from radioligands bound to SSTR positive BC cells can also affect neighboring low STTR2-expressing or SSTR2 negative cells. Furthermore, imaging studies performed prior to therapy can determine heterogeneity of SSTR2 expression of tumors prior to treatment. In addition, therapy with the antagonist could potentially be used for tumor shrinkage, even in heterogeneous tumors, after which other therapies could be applied.

In a study by Dude et al. (*21*), uptake of 2 SSTR agonists (DOTATOC and DOTA-Tyr^3-octreotate) and 1 SSTR antagonist (NODAGA-JR11) was compared in a BC xenograft model (ZR75-1). The authors reported a higher uptake of ^{68}Ga-DOTATOC versus ^{68}Ga-NODAGA-JR11, while the uptake of ^{68}Ga-NODAGA-JR11 was higher than that of ^{68}Ga-DOTA-Tyr^3-octreotate which is in line with our findings. This indicates that SSTR antagonists might not always be superior to agonists for tumor targeting. This could be explained by the different affinity of DOTATOC for SSTR subtypes compared to NODAGA-JR11 and DOTA-Tyr^3-octreotate. Additional studies are needed to determine the role of SSTR subtype expression in order to choose the optimal radiotracer for targeting of BC.

In conclusion, we demonstrated the advantage of radiolabeled SSTR antagonists versus agonists for BC targeting in a preclinical setting, shedding new light on SSTR-mediated BC imaging. The application of an SSTR antagonist, combined with other recent developments, including dedicated breast cameras (*22*) and PET radionuclides (*23*), is very promising and might result in a (more) important role for SSTR-mediated imaging (and treatment) of BC patients.

REFERENCES

1. Reubi JC, Waser B, Foekens JA, Klijn JG, Lamberts SW, Laissue J. Somatostatin receptor incidence and distribution in breast cancer using receptor autoradiography: relationship to EGF receptors. *Int J Cancer.* 1990;46:416-420.

2. Dalm SU, Melis M, Emmering J, Kwekkeboom DJ, de Jong M. Breast cancer imaging using radiolabelled somatostatin analogues. *Nucl Med Biol.* 2016;43:559-565.

3. Ginj M, Zhang H, Waser B, et al. Radiolabeled somatostatin receptor antagonists are preferable to agonists for in vivo peptide receptor targeting of tumors. *Proc Natl Acad Sci U S A.* 2006;103:16436-16441.

4. Cescato R, Waser B, Fani M, Reubi JC. Evaluation of 177Lu-DOTA-sst2 antagonist versus 177Lu-DOTA-sst2 agonist binding in human cancers in vitro. *J Nucl Med.* 2011;52:1886-1890.

5. Wild D, Fani M, Behe M, et al. First clinical evidence that imaging with somatostatin receptor antagonists is feasible. *J Nucl Med.* 2011;52:1412-1417.

6. Dalm SU, Nonnekens J, Doeswijk GN, et al. Comparison of the therapeutic response to treatment with a 177Lu-labeled somatostatin receptor agonist and antagonist in preclinical models. *J Nucl Med.* 2016;57:260-265.

7. Wild D, Fani M, Fischer R, et al. Comparison of somatostatin receptor agonist and antagonist for peptide receptor radionuclide therapy: a pilot study. *J Nucl Med.* 2014;55:1248-1252.

8. Reubi JC, Waser B, Macke H, Rivier J. Highly increased 125I-JR11 antagonist binding in vitro reveals novel indications for sst2 targeting in human cancers. *J Nucl Med.* 2017;58:300-306.

9. de Blois E, Chan HS, de Zanger R, Konijnenberg M, Breeman WA. Application of single-vial ready-for-use formulation of 111In- or 177Lu-labelled somatostatin analogs. *Appl Radiat Isot.* 2014;85:28-33.

10. Van Den Bossche B, D'Haeninck E, De Vos F, et al. Oestrogen-mediated regulation of somatostatin receptor expression in human breast cancer cell lines assessed with 99mTc-depreotide. *Eur J Nucl Med Mol Imaging.* 2004;31:1022-1030.

11. Kumar U, Grigorakis SI, Watt HL, et al. Somatostatin receptors in primary human breast cancer: quantitative analysis of mRNA for subtypes 1--5 and correlation with receptor protein expression and tumor pathology. *Breast Cancer Res Treat.* 2005;92:175-186.

12. Dalm SU, Sieuwerts AM, Look MP, et al. Clinical relevance of targeting the gastrin-releasing peptide receptor, somatostatin receptor 2, or chemokine c-x-c motif receptor 4 in breast cancer for imaging and therapy. *J Nucl Med.* 2015;56:1487-1493.

13. Marangoni E, Vincent-Salomon A, Auger N, et al. A new model of patient tumor-derived breast cancer xenografts for preclinical assays. *Clin Cancer Res.* 2007;13:3989-3998.

14. Fani M, Braun F, Waser B, et al. Unexpected sensitivity of sst2 antagonists to N-terminal radiometal modifications. *J Nucl Med.* 2012;53:1481-1489.

15. Reubi JC, Schar JC, Waser B, et al. Affinity profiles for human somatostatin receptor subtypes SST1-SST5 of somatostatin radiotracers selected for scintigraphic and radiotherapeutic use. *Eur J Nucl Med.* 2000;27:273-282.

16. van Eerd JE, Vegt E, Wetzels JF, et al. Gelatin-based plasma expander effectively reduces renal uptake of 111In-octreotide in mice and rats. *J Nucl Med.* 2006;47:528-533.

17. Rolleman EJ, Valkema R, de Jong M, Kooij PP, Krenning EP. Safe and effective inhibition of renal uptake of radiolabelled octreotide by a combination of lysine and arginine. *Eur J Nucl Med Mol Imaging.* 2003;30:9-15.

18. Stewart FA, Akleyev AV, Hauer-Jensen M, et al. ICRP publication 118: ICRP statement on tissue reactions and early and late effects of radiation in normal tissues and organs--threshold doses for tissue reactions in a radiation protection context. *Ann ICRP.* 2012;41:1-322.

19. de Jong M, Krenning E. New advances in peptide receptor radionuclide therapy. *J Nucl Med.* 2002;43:617-620.

20. Strosberg J, El-Haddad G, Wolin E, et al. Phase 3 trial of 177Lu-dotatate for midgut neuroendocrine tumors. *N Engl J Med.* 2017;376:125-135.

21. Dude I, Zhang Z, Hundal N, et al. Preclinical evaluation of somatostatin receptor agonist versus antagonist radioligands for breast cancer imaging. *J Nucl Med.* 2016;57 (Supplement 2):1175 [abstract]

22. Vercher-Conejero JL, Pelegri-Martinez L, Lopez-Aznar D, Cozar-Santiago Mdel P. Positron emission tomography in breast cancer. *Diagnostics (Basel).* 2015;5:61-83.

23. Buchmann I, Henze M, Engelbrecht S, et al. Comparison of 68Ga-DOTATOC PET and 111In-DTPAOC (Octreoscan) SPECT in patients with neuroendocrine tumours. *Eur J Nucl Med Mol Imaging.* 2007;34:1617-1626.

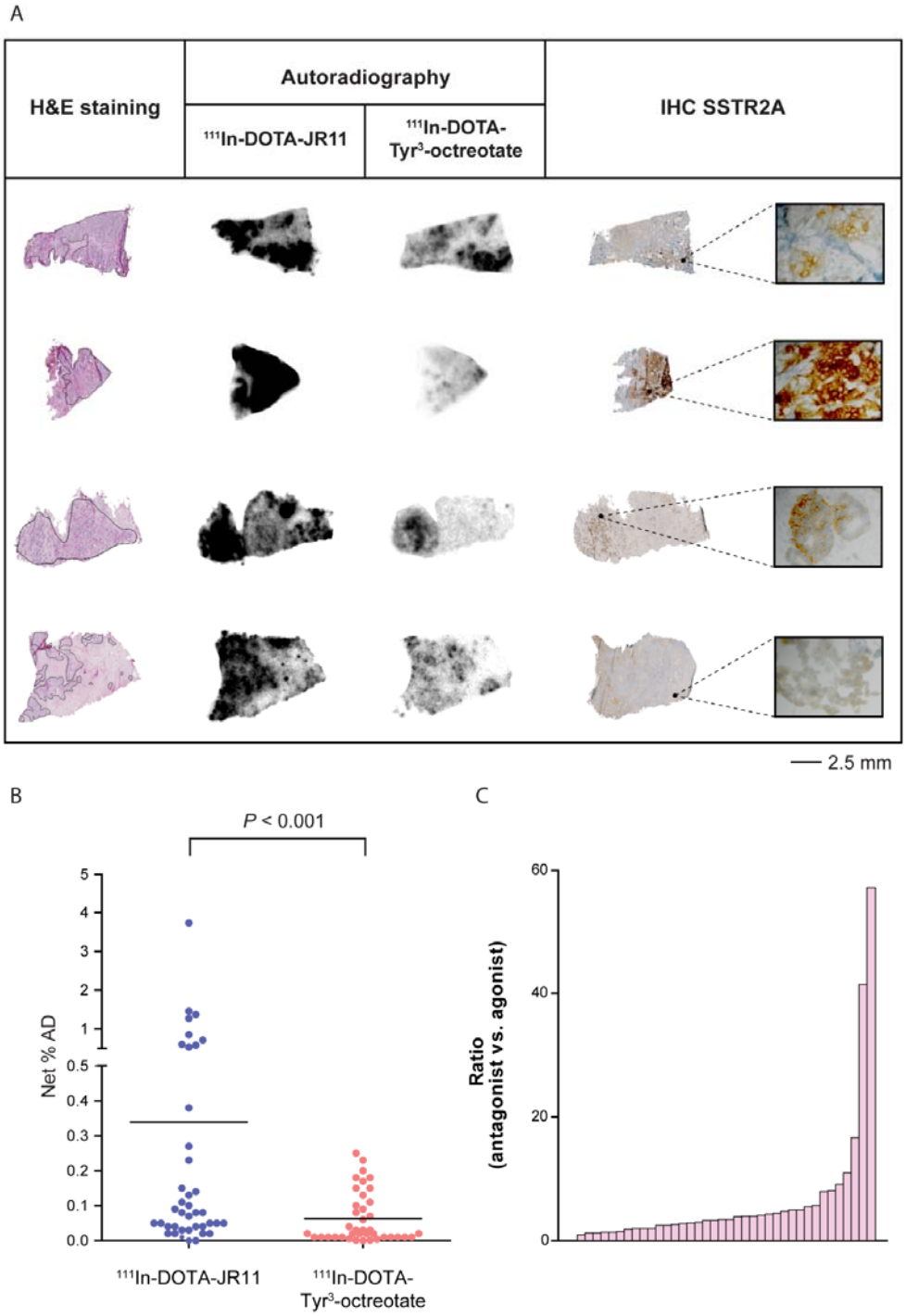

Figure 1. A. Representative autoradiography results performed with ^{111}In-DOTA-JR11 and ^{111}In-DOTA-Tyr^3-octreotate. Hematoxylin and eosin (H&E) staining and SSTR2-immunostaining was performed on adjacent tissue sections indicating tumor cells and SSTR2 expression, respectively. B. Quantified uptake (Net %AD, corrected for unspecific binding) of

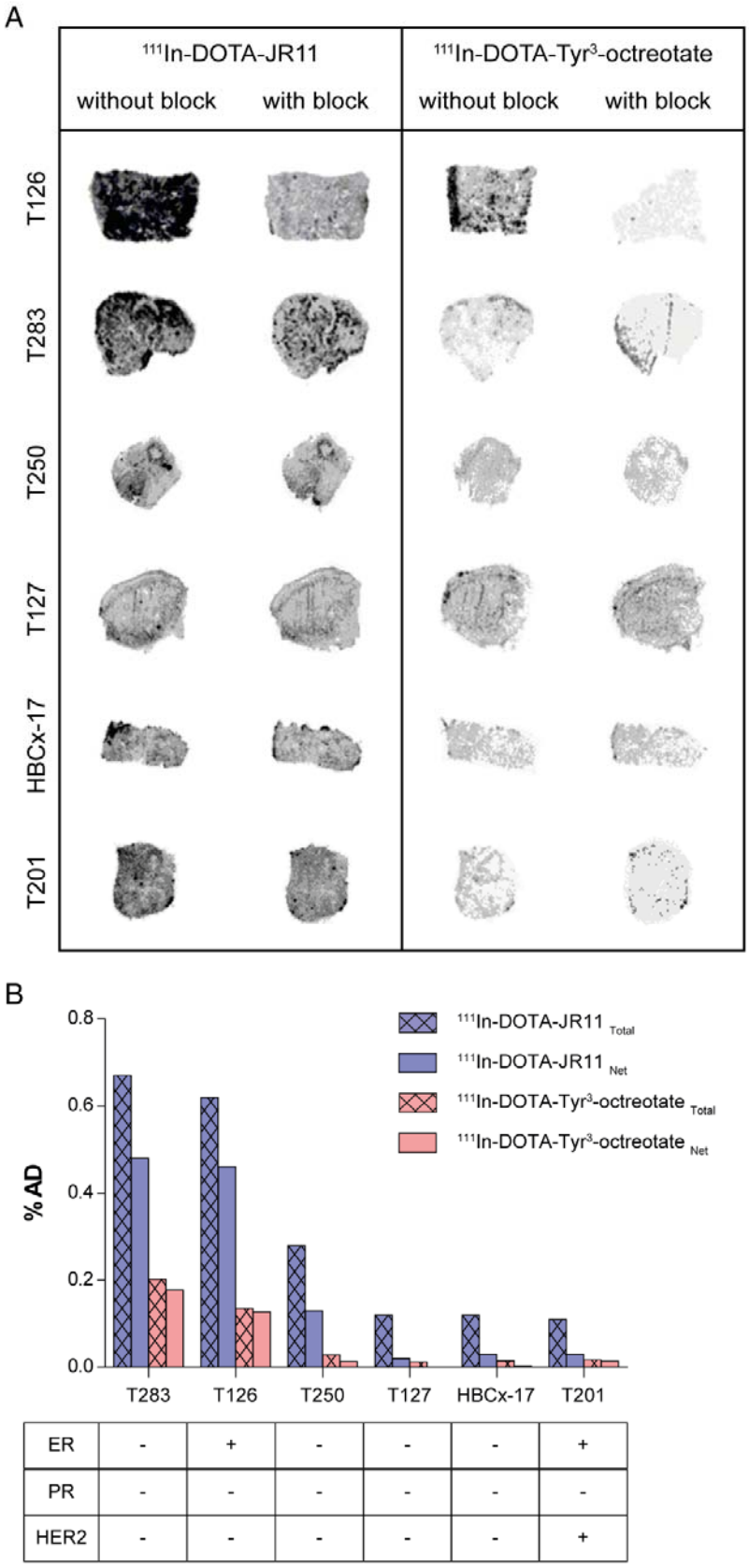

	T283	T126	T250	T127	HBCx-17	T201
ER	-	+	-	-	-	+
PR	-	-	-	-	-	-
HER2	-	-	-	-	-	+

Figure 2. A. Autoradiography results (without and with an excess of unlabeled octreotide to determine specificity of binding) of tumor material from 6 pdx's. Scaling was similar for agonist and antagonist binding to the same pdx, but not for the different pdx's. Therefore uptake between the different pdx's cannot be compared based on the images. Tumor sections with very low radioligand binding (blocked tumor section of pdx T283 and T201) are color corrected to enable visualization and may not correctly correlate with the measured quantified uptake displayed in part B of the figure. B. Quantified uptake (Total percentage of the added dose (Total %AD) and Net percentage of added dose (Net %AD) corrected for unspecific binding) of ^{111}In-DOTA-JR11 and ^{111}In-DOTA-Tyr^3-octreotate of the autoradiography displayed in A. The ER, PR and HER2 status of the pdx models is displayed in the table.

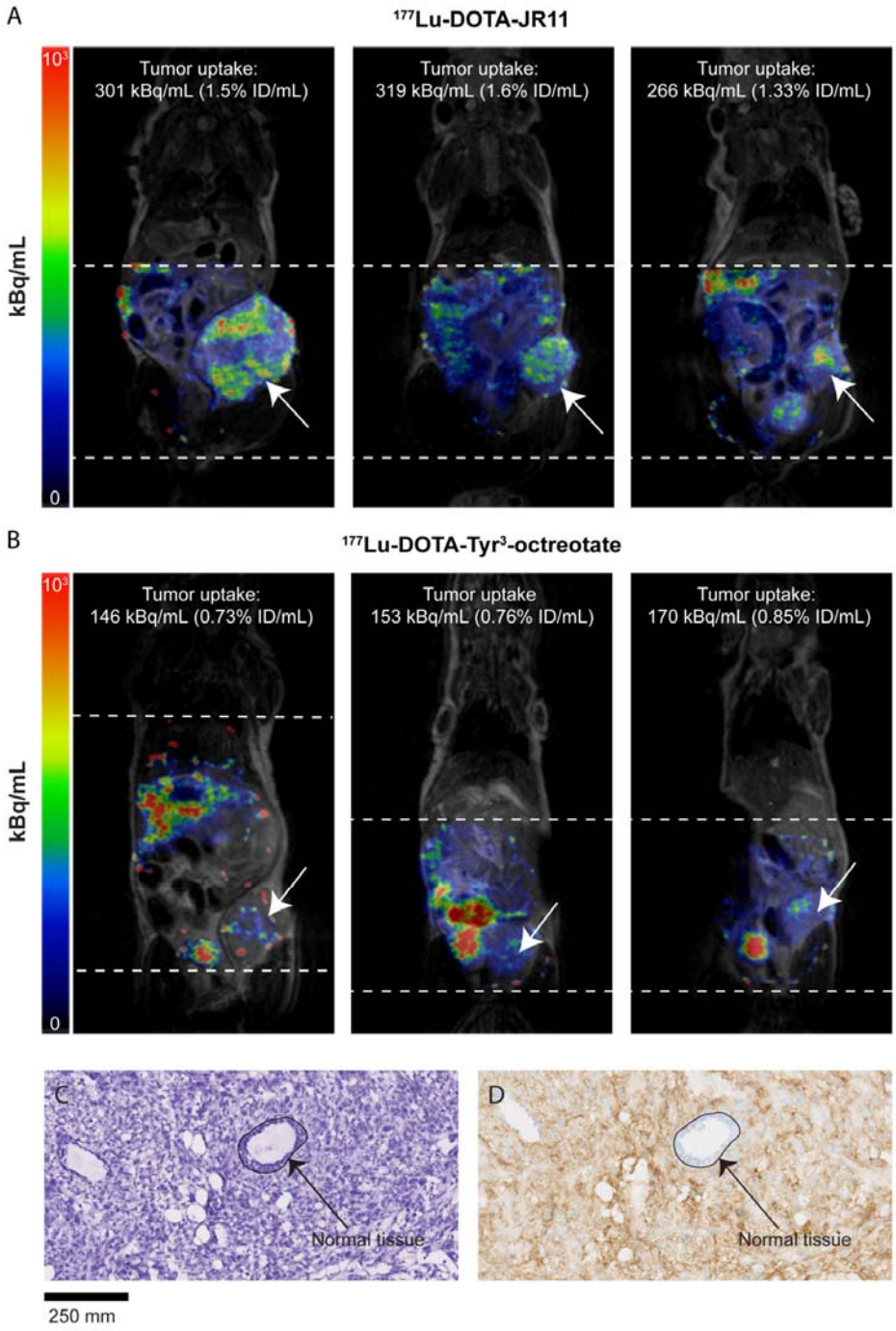

Figure 3. SPECT/MR images and quantified tumor uptake post injection of ^{177}Lu-DOTA-JR11 (A) and ^{177}Lu-DOTA-Tyr^{3}-octreotate (B). Scales are equal for all images. The dotted lines indicate the area scanned with SPECT. Arrows indicate tumor xenografts. C+D. H&E and SSTR2-immunostaining of excised tumors showing SSTR2 expression. Arrows indicate normal tissue (epithelial lining of a duct) without SSTR2 expression.

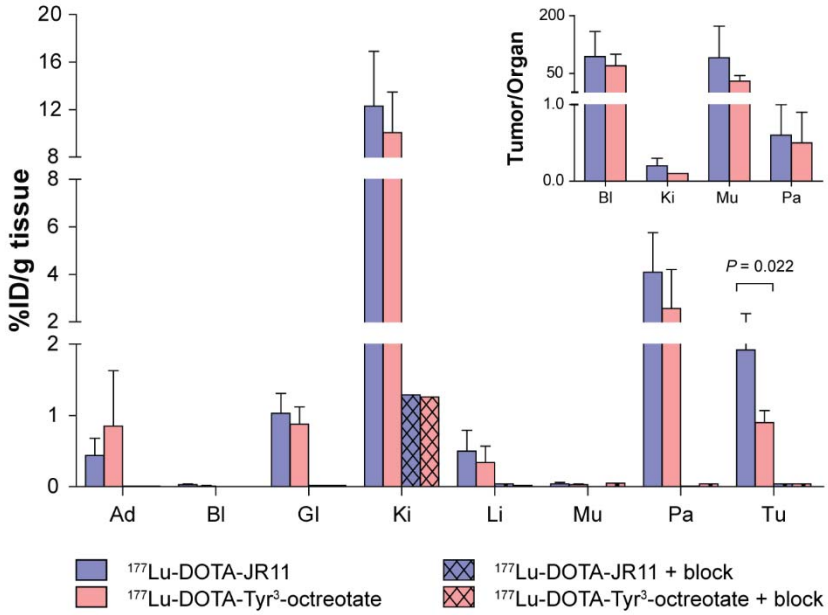

Figure 4. E. Radioactivity uptake (%ID/g tissue) measured in excised tumors and organs after imaging studies were performed. In addition, blocking studies were performed by injection of the radiotracers plus an excess of the unlabeled peptide analogs. Tumor to organ ratios are displayed in the right upper corner. Ad=adrenals, Bl=blood, GI=GI-tract, Ki=kidney, Li=liver, Mu=muscle, Pa=pancreas and Tu=tumor.

TABLES

Table 1. Somatostatin receptor affinity of DOTA-JR11 and DOTA-Tyr^3-octreotate

	SSTR1	**SSTR2**	**SSTR3**	**SSTR4**	**SSTR5**
DOTA-JR11*	> 1,000	0.72±0.12	>1,000	>1,000	>1,000
DOTA-Tyr^3-octreotate†	>10,000	1.5±0.4	>1,000	453±176	547±160

** Data published by Fani et al. (14)*

† Data published by Reubi et al. (15)

Table 2. Results of SSTR2-immunostaining.

	Weak	**Moderate**	**Strong**	**Total**
Heterogeneous	16 %	8 %	5 %	**30 %**
Homogenous	35 %	8 %	27 %	**70 %**
Total	**51 %**	**16 %**	**32 %**	